Journal of the Mechanics and Physics of Solids 58 (2010) 2083–2099

Contents lists available at ScienceDirect

Journal of the Mechanics and Physics of Solids

journal homepage: www.elsevier.com/locate/jmps

A thermodynamic model of physical gels

Yonghao An [a], Francisco J. Solis [b], Hanqing Jiang [a,*]

[a] School for Engineering of Matter, Transport, and Energy, Arizona State University, Tempe, AZ 85287, USA
[b] Division of Mathematical and Nature Sciences, Arizona State University, Phoenix, AZ 85069, USA

ARTICLE INFO

Article history:
Received 23 June 2010
Received in revised form
31 August 2010
Accepted 5 September 2010

Keywords:
Physical gels
Free energy
Thermodynamics
Reformation
Phase transition

ABSTRACT

Physical gels are characterized by dynamic cross-links that are constantly created and broken, changing its state between solid and liquid under influence of environmental factors. This restructuring ability of physical gels makes them an important class of materials with many applications, such as in drug delivery. In this article, we present a thermodynamic model for physical gels that considers both the elastic properties of the network and the transient nature of the cross-links. The cross-links' reformation is captured through a connectivity tensor **M** at the microscopic level. The macroscopic quantities, such as the volume fraction of the monomer ϕ, number of monomers per cross-link s, and the number of cross-links per volume q, are defined by statistic averaging. A mean-field energy functional for the gel is constructed based on these variables. The equilibrium equations and the stress are obtained at the current state. We study the static thermodynamic properties of physical gels predicted by the model. We discuss the problems of un-constrained swelling and stress driven phase transitions of physical gels and describe the conditions under which these phenomena arise as functions of the bond activation energy E_a, polymer/solvent interaction parameter χ, and external stress p.

1. Introduction

Gels are materials where polymer chains form the links of a network immersed in a typically liquid environment. The polymer chains are cross-linked at the microscopic level by chemical bonds or weaker physical bonds; the type of bond is used to label the macroscopic material as a chemical or a physical gel, respectively. The physical bonds can have diverse origins, such as van der Waals interactions or hydrogen bonding, and can involve a complex local structure such as the formation of a small crystalline domain. Because of their significant liquid content (up to 99% liquid by weight), often comparable to conditions in physiological tissue, gels have found various applications, especially in biomedical contexts. For example, gels are used as scaffolds in tissue engineering (Lee and Mooney, 2001; Lee et al., 2006; Beck et al., 2007), as systems of sustained drug delivery (Jeong et al., 1997; Qiu and Park, 2001), as materials for contact lenses, and in many stimuli-sensitive actuators (Beebe et al., 2000; Sidorenko et al., 2007). In the rational design of the materials required for these applications, knowledge and prediction of key properties are crucial. It is therefore highly desirable to have specific models for these materials capable of describing their response to external stimuli.

The different microscopic behaviors of cross-links in chemical and physical gels endow them with distinct macroscopic properties. Since the chemical cross-links prevent the chemical gels from dissolving in its environment solvent, chemical

* Corresponding author.
E-mail address: hanqing.jiang@asu.edu (H. Jiang).

0022-5096/$ - see front matter © 2010 Elsevier Ltd. All rights reserved.
doi:10.1016/j.jmps.2010.09.002

gels behave macroscopically like solids. However, because of the weaker nature of the cross-linking bonds, physical cross-links are found in a constant cycle of creation and dissolution in physical gels. At short time scales, against quick deformation, the cross-links do not have time to dissolve and the gel shares the same solid-like behavior of chemical gels. At long time scales, bond destruction is able to eventually release all shear or anisotropic stress. In other words, physical gels can adapt to the presence of boundaries in much similar way as a liquid at long time scales.

Physical gels exhibit important thermally driven properties. Their phase diagram can contain a reversible solution–gel (i.e., sol–gel) transition within the range of temperatures of the host fluid (water in most cases). These transitions are particularly useful in applications when the materials exhibit a lower critical solution temperature (LCST). In this case the polymer is in solution at low temperatures and becomes gel at a higher temperature (Ono et al., 2007). These materials can be deployed in biomedical applications as injectable polymers, liquid at room temperature but forming a gel at physiological temperature. Therefore, physical gels are sometimes called thermoreversible gels, i.e., the creation and dissolution of cross-links or sol–gel transition are temperature driven and reversible.

Theoretical models for the thermodynamic behavior of chemical gels have been extensively studied. Many of these models are based on Flory–Huggins solution theory (Flory, 1941, 1942; Huggins, 1941). Recently, Hong et al. (2008) have developed a rigorous framework to describe the coupled large deformation and diffusion in chemical gels. The solid-like property of chemical gels makes it feasible to use the concept of "markers" that are commonly used in solid mechanics to describe the deformation from one configuration (with position $\mathbf{X}$) to another (with position $\mathbf{x}(\mathbf{X},t)$). By tracking the trajectory of the markers upon deformation in the Lagrangian description, the macroscopic deformation gradient $\mathbf{F}=\partial\mathbf{x}(\mathbf{X},t)/\partial\mathbf{X}$ can be defined and the stress tensor at the macroscopic level is just the work conjugate with respect to the deformation gradient $\mathbf{F}$. The kinetic law of diffusion follows the Fickian model and was presented in a rigorous manner by differentiating the different configurations.

In contrast, the microscopic characteristics of physical gels, i.e., the creation and dissolution of cross-links lead to new forms of macroscopic behaviors. The "markers" can still be used but the microscopic characteristic associated with them change. The connectivity of the cross-links at the microscopic level becomes an *independent internal degree of freedom*. Their connectivity is not solely governed by the deformation from a reference state but also depends on its own evolution rule. Therefore, the stress cannot be solely determined by the deformation; it also depends on the continuous reconstruction of the network which "fades out" the deformation history. More precisely, the stress of the materials is a function of its instantaneous connectivity at the current state.

This paper develops a phenomenological model for physical gels that emphasizes internal variables that describe both the density of cross-links and their spatial organization. We obtain a mean field model of the thermodynamic properties of the physical gels. Fig. 1 illustrates some of the properties of the model. At the microscopic level, we define a connectivity tensor to describe the local environment of the cross-links. When the reformation of cross-links occurs, the neighbors of a cross-link and the intrinsic length of the linking polymer segments change, which alters the connectivity tensor. Therefore, the connectivity tensor can capture the reformation of the cross-links at this level. We formulate a macroscopic free energy density function based on the mean-field model and the description of the gel through the connectivity tensor. We propose a model for the dynamics of the connectivity of cross-links that explicitly considers the evolution of the cross-links. We use standard thermodynamic notation (e.g., Prigogine, 1967) as well as some terminology from Hong et al. (2008).

The structure of the paper is the following. Section 2 defines the connectivity tensor and its counterpart under statistical average. A kinetic law for the evolution of cross-links is also given in this section. Section 3 formulates a mean-field free energy density function. The equilibrium equations are derived in Section 4, while the explicit form of the macroscopic

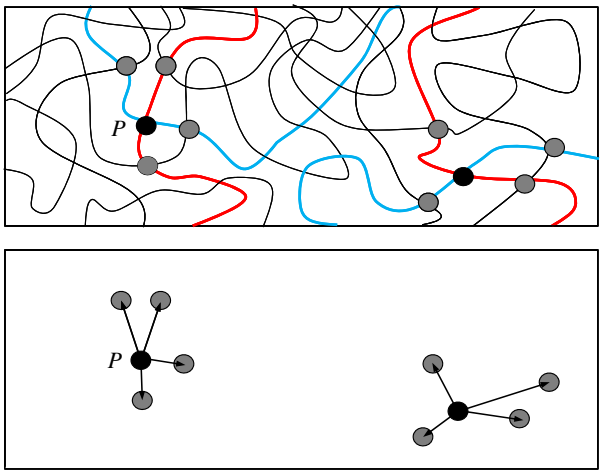

Fig. 1. The scheme shows a gel formed by a set of polymers. Contacts between pairs of polymers can lead to the formation of cross-links; a subset of these cross-links is indicated with filled circles. The scheme shows two examples of pairs of polymers chains, marked red and blue, that form a cross-link here shown as a black circle. These cross-links have four neighboring cross-links marked with grey circles. The bottom panel shows the relative vectors of position for the neighbors of these cross-links. These vectors are used to define the connectivity tensor as explained in the text. (For interpretation of the references to colour in this figure legend, the reader is referred to the web version of this article.)

stress tensor is obtained in Section 5. Section 6 discusses the physical range of values of key parameters. Section 7 analyzes the un-constrained swelling of a physical gel, while a stress driven phase transition is studied in Section 8, followed by concluding remarks of this paper in Section 9. The two appendices show that this model degenerates to the case of chemical gels when the cross-links become fixed.

2. Field variables: connectivity tensor, number density of monomers, and number of monomers per cross-link

2.1. Microscopic level

As shown in Fig. 1, at the microscopic level, polymer chains are cross linked by physical cross-links, marked as filled circles. These cross-links are randomly distributed in space. In the most common cases, the cross-links have four nearest-neighbor cross-links.[1] For example, cross-link P joins the red and blue polymer chains and has a pair of nearest neighbors in each chain (top panel). Define four linking vectors, $\mathbf{R}^{P_n}$ $(n=1,2,3,4)$ that emanate from the cross-link P and end at the four neighboring cross-links (bottom panel). Thus, these four linking vectors can reflect the local distribution of cross-links at microscopic level. This definition can be applied to any cross-links. At the cross-link P, a symmetric and positive definite connectivity tensor $\mathbf{M}^P$ is defined by these linking vectors as

$$M_{ij}^P = \frac{1}{4}\sum_{n=1}^{4} R_i^{P_n} R_j^{P_n}. \tag{1}$$

The dynamics of the cross-links alters the number of monomers between two cross-links along a polymer chain. Similar to the case of the linking vectors $\mathbf{R}^{P_n}$, the number of monomers allocated to a cross-link, such as P, is defined as the following average:

$$s^P = \frac{1}{4}\sum_{n=1}^{4} s^{P_n}, \tag{2}$$

where $s^{P_n}(n=1,2,3,4)$ is the number of monomers along nth branch of a polymer chain emanating from P and ending at the corresponding neighboring cross-links. It should be noted that the linking vectors $\mathbf{R}^{P_n}$ (or the connectivity tensor $\mathbf{M}^P$) and the number of monomers s^P are independent, because $\mathbf{R}^{P_n}$ describes the geometric distribution of monomers in space, while s^P gives information of mass distribution of monomers.

2.2. Macroscopic level

The connectivity tensor $\mathbf{M}$ at a material particle (or a marker) is the statistic average of its counterpart at the microscopic level. This average leads to a macroscopic connectivity tensor

$$M_{ij} = \langle M_{ij}^P \rangle. \tag{3}$$

The trace of $\mathbf{M}$ represents the average square of link–link distance at a material particle

$$M_{kk} = \left\langle \frac{1}{4}\sum_{i=1}^{4} (R^{P_n})^2 \right\rangle. \tag{4}$$

Similarly, at each material particle, the average number of monomers allocated to a cross-link is the statistic average of its microscopic variables

$$s = \langle s^P \rangle. \tag{5}$$

Thus, the connectivity tensor $\mathbf{M}$ and average number of monomers s allocated to a cross-link form continuum fields, $\mathbf{M}(\mathbf{x}, t)$ and $s(\mathbf{x}, t)$, that evolve with time and characterize the dynamics of the cross-links.

2.2.1. Isotropic state

The isotropic state is an ideal state in which the probability of finding nearest-neighbor cross-links of a given cross-link is the same along any spatial direction. In other words, the local environment for all cross-links is identical.

The macroscopic connectivity tensor $\mathbf{M}_o$ for an isotropic state is proportional to the identity tensor

$$\mathbf{M}_o = \frac{1}{3}R_o^2 \begin{bmatrix} 1 & 0 & 0 \\ 0 & 1 & 0 \\ 0 & 0 & 1 \end{bmatrix}, \tag{6}$$

where R_o is the statistic average of the length of linking vectors, and the subscript "o" denotes the isotropic state.

[1] Here we do not consider the rare situations in which the cross-links do not have four nearest-neighbor crosslinks, such as the case when the crosslinking agent requires the simultaneous presence of more than two chains to produce the association or the links are created at extremes of the chains with finite length. We assume that these rare cases are not statistically significant for the model.

We assume that in the isotropic state the local level connectivity structure is similar to that of the diamond lattice structure. In both cases the repeated unit (the atom of diamond structure and the cross-link of the gel network) has a coordination number 4. They both lead, upon averaging, to isotropic connectivity tensors and have equal distances between nearest neighbors. Derived quantities such as the density of cross-links are therefore calculated in the isotropic state using the information for the diamond lattice. The number density of cross-links is equivalent to the number density of atoms in the diamond structure and is given by

$$q_o = \frac{3\sqrt{3}}{8R_o^3}. \tag{7}$$

The number density of monomers allocated to each cross-link is

$$\phi_o = \frac{3\sqrt{3}s_o}{4R_o^3}, \tag{8}$$

where s_o is the average number of monomers between two cross-links. Other representative structures can be used instead of the diamond lattice structure. A different choice of structure will lead to different prefactors in Eqs. (7) and (8) but lead to the same qualitative properties of the model.

2.2.2. Arbitrary state

In general, the deformations of the gel lead to non-isotropic inhomogeneous states. In the following, we establish the relations between the connectivity tensor in an arbitrary state and the isotropic state.

The symmetry and positive definiteness of the connectivity tensor $\mathbf{M}$ allows its construction, for an arbitrary state, by means of a series of orthogonal transformations applied to a reference isotropic state that has the same density of cross-links. We write

$$\mathbf{M} = \mathbf{Q}\cdot\mathbf{D}\cdot\mathbf{M}'_o\cdot\mathbf{D}\cdot\mathbf{Q}^T = \mathbf{T}\cdot\mathbf{M}'_o\cdot\mathbf{T}^T, \tag{9}$$

where $\mathbf{Q}$ is an orthogonal tensor, $\mathbf{D}$ is diagonal and $\mathbf{M}'_o$ is isotropic. We can choose $\mathbf{D}$ to have determinant $|\mathbf{D}|=1$. Then we can write

$$\mathbf{M}'_o = \frac{1}{3}(R'_o)^2\begin{bmatrix}1&0&0\\0&1&0\\0&0&1\end{bmatrix}, \tag{10}$$

where R'_o is the average length of linking vectors at the reference isotropic state. $\mathbf{T}$ is the equivalent transformation tensor that maps the reference isotropic state to an arbitrary state. Therefore, at least locally, the connectivity tensor for an arbitrary state can be mapped to that of a reference isotropic state by means of affine transformations. During the affine transformations the number of monomers in a reference region is not changed even as the total volume does. The affine transformations do no modify the number of cross-links of the region either.

It should be emphasized that, in general, an arbitrary state cannot be mapped, using the previous transformation, from the physical isotropic initial state since the number of cross-links may be different, as illustrated in Fig. 2. However, any arbitrary state can be geometrically mapped from a reference isotropic state while preserving number of cross-links. For each arbitrary state there is a corresponding reference isotropic state. Although reference states are usually chosen as stress-free states in continuum mechanics, it is not required that the reference state in this problem be an actual physical state of the body. The reference state can have a conceptual nature.

In Eq. (9), tensor $\mathbf{T}$ geometrically maps an infinitesimal vector $d\mathbf{X}'$ defined in a reference isotropic state to $d\mathbf{x}$ in an arbitrary state by

$$d\mathbf{x} = \mathbf{T}\cdot d\mathbf{X}'. \tag{11}$$

Since the reference isotropic state and the arbitrary state have the same number of cross-links, the tensor $\mathbf{T}$ has the same properties as the deformation gradient $\mathbf{F}$ in continuum mechanics. An infinitesimal element in the reference isotropic state with volume dV'_o changes, upon deformation, to dv in the arbitrary state. The ratio of the volumetric change is given

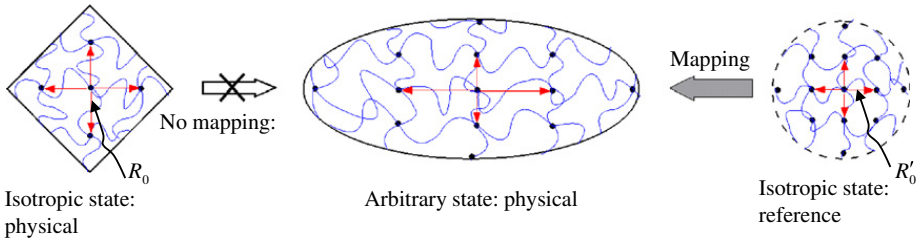

Fig. 2. Mappings between physical or reference isotropic states and arbitrary state. The reference isotropic state has different average length of linking vectors, marked as R'_0 compared with R_0 for the physically isotropic state. The mapping is only possible if the number of cross-links is preserved by the transformation.

by the determinant of the transformation tensor **T**

$$\det\mathbf{T}=\frac{dv}{dV'_o}. \tag{12}$$

which we have chosen to be $\det|\mathbf{T}|=1$. The number of monomers is conserved during this affine transformation and we can simply use their density in the reference isotropic state. Combining with Eq. (8), we can write the number density of monomers in the arbitrary state as

$$\phi=\frac{s}{4\sqrt{\det\mathbf{M}}}. \tag{13}$$

Similarly, the number density of cross-links can be related to **M** as

$$q=\frac{\phi}{2s}=\frac{1}{8\sqrt{\det\mathbf{M}}}. \tag{14}$$

2.3. Dynamic evolution of field variables

The evolution of the monomer density ϕ and the connectivity tensor **M** can be modeled on the basis of fairly general properties of the system as described below. We note that the previous relation given for the average link length s in terms of our independent variables fully determines its dynamics once the evolution rules for those variables are specified.

2.3.1. Evolution of ϕ

The evolution of ϕ is governed by the mass conservation law

$$\frac{\partial\phi}{\partial t}+\frac{\partial(\phi v_i^p)}{\partial x_i}=0,$$

where v_i^p is the absolute velocity of the polymer network. We assume that v_i^p approximates the relative velocity of the polymer network with respect to the solvent v_i by taking the solvent as a fixed background. Without loss of the physical generality, this assumption can lead to a completed scheme by latterly relating v_i with the stress of gel through the conservation of the linear momentum (Eq. (39)).

2.3.2. Evolution of **M**

We consider two different forms of transformation of the connectivity tensor **M**.

(1) *Deformation induced evolution of* **M**

First we discuss the affine transformations induced by macroscopic deformations of the gel. In these transformations the cross-links are preserved. An example of the effect of this type of transformation appears in Fig. 3a. At time t, a material particle occupies a position with coordinate **x**. At time $t+\Delta t$, this material particle is found at position $\tilde{\mathbf{x}}$ after a displacement $\Delta\mathbf{x}$

$$\tilde{\mathbf{x}}=\mathbf{x}+\Delta\mathbf{x}. \tag{15}$$

With the displacement field $\Delta\mathbf{x}$, the linking vector **R** is mapped to a new value$\tilde{\mathbf{R}}$ as

$$\tilde{\mathbf{R}}=\mathbf{f}\cdot\mathbf{R}, \tag{16}$$

where **f** maps between two configurations with the same cross-links

$$f_{ij}=\delta_{ij}+\frac{\partial\Delta x_i}{\partial x_j}. \tag{17}$$

The increment of displacement field $\Delta\mathbf{x}$ also leads to the infinitesimal strain

$$\varepsilon_{ij}=\frac{1}{2}\left[\frac{\partial(\Delta x_i)}{\partial x_j}+\frac{\partial(\Delta x_j)}{\partial x_i}\right]. \tag{18}$$

The connectivity tensor **M** at time $t+\Delta t$ is obtained from its value at time t as

$$\tilde{\mathbf{M}}=\mathbf{f}\cdot\mathbf{M}\cdot\mathbf{f}^T. \tag{19}$$

The rate of change of the connectivity tensor **M** due to deformation $\Delta\mathbf{x}$ is then given by

$$\left.\frac{d\mathbf{M}}{dt}\right|_{deformation}=2\frac{d\boldsymbol{\varepsilon}}{dt}\cdot\mathbf{M} \tag{20}$$

where we have used the symmetry properties of the tensor and the relation between the rates **f** and $\boldsymbol{\varepsilon}$

$$\frac{d\mathbf{f}}{dt}=\frac{d\boldsymbol{\varepsilon}}{dt}\cdot\mathbf{f}. \tag{21}$$

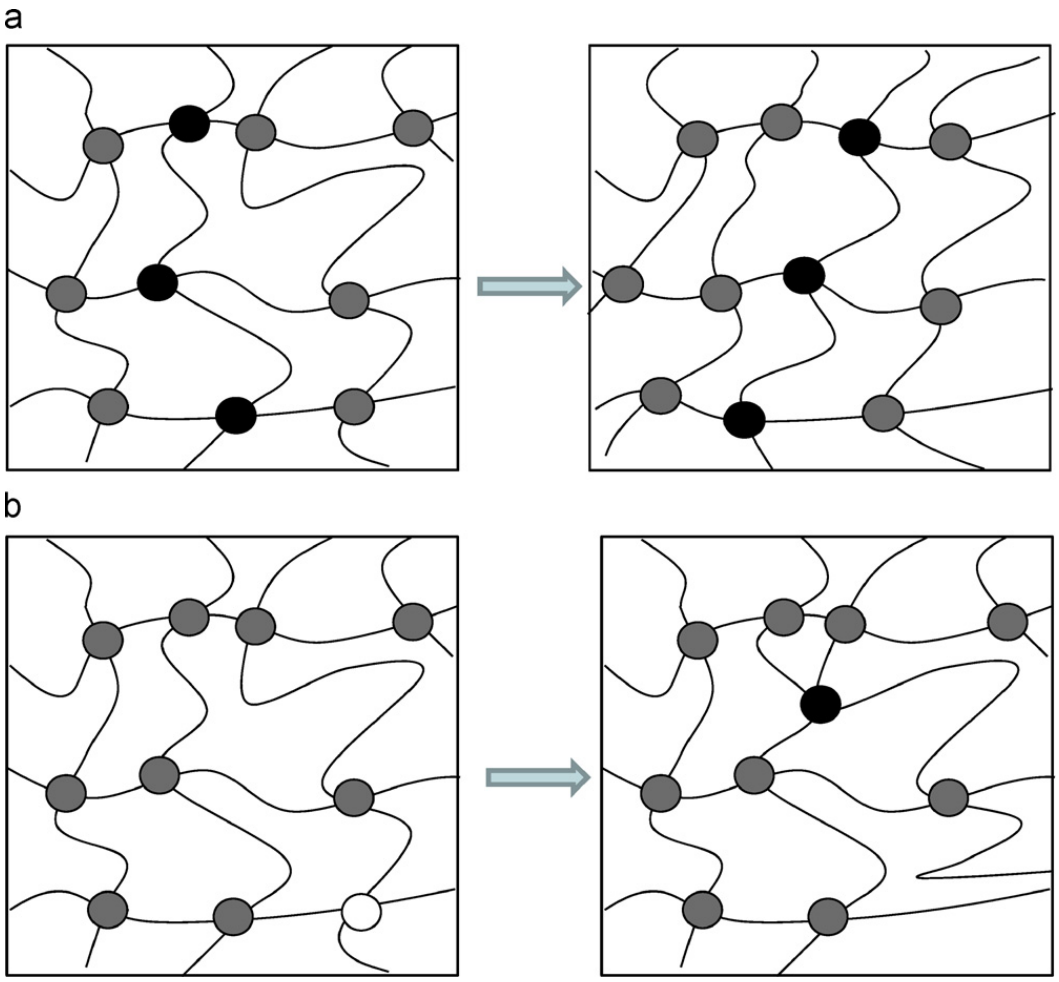

Fig. 3. Scheme of the two types of dynamical transformations considered by the model. (a) The gel undergoes an affine transformation where the average positions of the cross-linkers are changed following a macroscopic displacement field. Black markers identify the same cross-links in both panels. (b) An example of reconstruction of the network: the white cross-link disappears while the black one is created.

(2) *Reconstruction induced evolution of* **M**

The dynamic nature of cross-links in physical gels permits their relaxation from arbitrary stress states to isotropic stress states. As the location of cross-links is dynamic, new cross-links can be formed at energetically favorable positions that reduce stress. Such processes are illustrated in Fig. 3b. Conversely, cross-links that impose connectivities that lead to unbalanced or excess stress become more likely to disappear. Both processes lead an arbitrary initial state into an isotropic stress final state. We assume the following phenomenological model to describe the evolution of the connectivity tensor **M** due to these network reconfigurations

$$\left.\frac{d\mathbf{M}}{dt}\right|_{reconstruction} = \frac{1}{\tau_{re}}(\mathbf{M} - m_\phi \mathbf{1}). \tag{22}$$

Here τ_{re} is the characteristic time for the reconstruction of the cross-links and $m_\phi\mathbf{1}$ is the *optimal* isotropic state depending on the number density of monomers ϕ at the current time t. We describe in the next section the construction of explicit expressions for the free energy W_{tot} of the system. The optimal value m_ϕ is determined by minimizing this total free energy. As discussed below, in Section 3, the free energy depends on **M** and ϕ, so that m_ϕ is a function of ϕ. Because ϕ changes with time, this desired isotropic state $m_\phi\mathbf{1}$ also evolves with time. In other words, during the dynamics evolution, this optimal isotropic state will not be reached, but provides a target or direction for the evolution. Only the last isotropic state can be realized.

The overall evolution of the connectivity tensor **M** is then given by

$$\frac{d\mathbf{M}}{dt} = 2\frac{d\boldsymbol{\varepsilon}}{dt}\cdot\mathbf{M} + \frac{1}{\tau_{re}}(\mathbf{M} - m_\phi 1). \tag{23}$$

A full description of the evolution of the gel requires complementary laws for the dynamics of the monomer concentration and the motion of the background fluid. The proposed dynamical description of the connectivity tensor can be incorporated into different schemes that describe the full gel. We note, in addition, that the idea that there exists at least two well differentiated processes during dynamic transformations of gels is well known, for both

chemical (Suzuki et al., 1999) and physical gels (Leon et al., 2009). Our proposed scheme identifies explicitly these two different mechanisms as the reconstruction of internal structure and the simpler affined deformations induced by motion of the boundaries of the system.

3. Free energy density function

We now consider the free energy density function W. Its integral over a volume v at the current state computes the total energy of the system due to the presence of the gel, i.e., $W_{tot}=\int_v W dv$. W consists of three contributions, the elastic energy of polymer chain $W_{elastic}$, the mixing energy of solvent and polymer W_{mix}, and the bond energy associated to the creation of cross-links W_{bond}, i.e.

$$W = W_{elastic} + W_{mix} + W_{bond}. \tag{24}$$

3.1. Elasticity energy density $W_{elastic}$

To describe the polymer segments between cross-links, we use the Gaussian chain model (Flory, 1953; Rubinstein and Colby, 2003). An unconstrained polymer segment composed by s monomers explores a number of states proportional to

$$\Omega_o = 2^{3s}, \tag{25}$$

i.e., the number of random walks of length s in a cubic lattice. When the segment correspond to a link in a gel, its extremes are constrained to occupy positions with relative length R; the number of states with such configuration is given by

$$\Omega = 2^{3s} P_{3d}(M_{kk},s) = 2^{3s}\left(\frac{3}{2\pi s}\right)^{3/2}\exp\left(-\frac{3M_{kk}}{2sb^2}\right), \tag{26}$$

where $P_{3d}(M_{kk}, s)$ is the probability distribution function of the end-to-end vector with distance $R(=\sqrt{M_{kk}})$ (Eq. (4)) of an ideal polymer chain of s monomers (Rubinstein and Colby, 2003), and b is the Kuhn length of monomer. The increase of entropy due to the constraint is then given by the standard thermodynamic computation

$$\Delta S = k\ln\Omega - k\ln\Omega_o = \frac{3}{2}k\ln 3 - \frac{3}{2}k\ln(2\pi s) - \frac{3kM_{kk}}{2sb^2}, \tag{27}$$

where k is Boltzmann's constant. The change of free energy per segment thus becomes

$$\Delta F = -T\Delta S = \frac{3}{2}kT\left[\ln(2\pi s) + \frac{M_{kk}}{sb^2} - \ln(3)\right], \tag{28}$$

where T is the temperature. Since the volume per monomer is $1/\phi$, and the volume associated with a link is s/ϕ, the elastic energy density is given by

$$W_{elastic} = \frac{\Delta F}{s/\phi} = \frac{3\phi kT}{2s}\left[\ln(2\pi s) + \frac{M_{kk}}{sb^2} - \ln(3)\right]. \tag{29}$$

Here the density of free energy is calculated with respect to the volume at the current state; instead of using the elastic energy per reference volume (Hong et al., 2008).

This formulation holds for both physical gels in which the number of monomers per chain s is a variable and chemical gels in which s is fixed and becomes a parameter. Appendix A shows that this elastic energy density can be presented in the standard format for chemical gels (Rubinstein and Colby, 2003).

3.2. Mixing energy density W_{mix}

Following Flory–Huggins' polymer solution theory (Rubinstein and Colby, 2003), the energy of mixing a s-monomer polymer chain and solvents is given by

$$\Delta W_{mix} = kT\left[\frac{c}{s}\ln c + (1-c)\ln(1-c) + \chi c(1-c)\right], \tag{30}$$

where c is the volume fraction of polymer, $1-c$ is the volume fraction of solvent, and χ is Flory's dimensionless parameter to describe the hydrophilicity of the polymer. The mixing energy density is thus the energy of mixing per unit lattice volume (i.e., the specific volume of a solvent molecule, v_s) by

$$W_{mix} = \frac{kT}{v_s}\left[(1-v_m\phi)\ln(1-v_m\phi) + \chi v_m\phi(1-v_m\phi)\right], \tag{31}$$

where v_m is the specific volume of a monomer unit.

In introducing this mixing energy term, we assume that all monomers are not involved in the bond formation with all other monomers and solvent molecules in a way that is properly described by a mean field theory. The interactions that

give rise to a gel forming bond are rare and these separate interactions are considered independently in the model and described in the next subsection.

3.3. Bond energy density W_{bond}

To describe the contribution of cross-links, we assume that they all have the same structure. We coarse-grain the details of the bonding interaction and simply write an effective free energy that assigns equal contribution to all of them

$$W_{bond} = -qE_a, \tag{32}$$

where $E_a(>0)$ is the activation energy or the energy required to disassociate a cross-link and q is the number density of the cross-links (see Eq. (14)).

We can further contrast the two different modes of interaction between monomers, namely generic polymer–polymer interactions in mixing energy and bond formation interactions in bond energy. One may consider a case in which the monomers can be found in two different states, one in which the interaction with other monomers is weak, and a second state where a bond can be formed. This scenario is discussed, for example, in Solis et al. (2005). Alternatively, the polymer might be constructed of two different monomers. The more abundant monomer has weak interactions with all other monomers, while a minority monomer can participate in bond formation. Both scenarios can be addressed through the same model. The main difference lies in the different values of number of monomers between two links, but these differences effectively disappear when we consider the value of s averaged over a large region. We also note that the experimental measurement of interaction parameter χ should be conducted for polymers only consisted of inert monomers in order to avoid possible overlap between the mixing and bond energies.

We note that if it is assumed that the bonding energy has an Arrhenius form, the activation energy E_a is related to the characteristic time τ_{re} for the reconstruction by

$$\tau_{re} = A\exp\left(\frac{E_a}{kT}\right), \tag{33}$$

where the prefactor A has dimensions of time and does not depend on temperature and activation energy. This simple model can be modified to include further details. For example, the activation energy E_a may contain an explicit temperature dependence to capture the LCST behavior.

The number density of cross-links q is a variable (given by Eq. (14)) for physical gels so that the bond energy density W_{bond} enters the picture. However for chemical gels, the cross-links are permanent and the number of monomers between two cross-links is fixed and q is just a parameter, such that the bond energy density W_{bond} is just a constant and does not enter the picture (or can be omitted in the free energy calculation).

3.4. Constraint of number of monomers between two cross-links

The components of the free energy density, $W_{elastic}$, W_{mix}, and W_{bond}, depend on two independent variables, such as $\mathbf{M}$ and ϕ; then the number of monomers between two cross-links, s, is determined according to Eq. (13). We note, however, that the mean-field theory presented has a limitation: the number of monomers between two cross-links cannot be indefinitely small. It is also consistent with the physical picture that the monomers capable of forming bonds are minority and there is lowest value of the average number of monomers in the chain segment between two nearest neighbored crosslinks. We only consider values such that $s \geq s_{lower}$. When the minimum of the free energy corresponds to smaller values of the link length, we consider that the gel is physically close to a dry state as there is relatively little space for the solvent. We implement this inequality and the relation to the independent variables using a Lagrange multiplier, and write

$$\overline{W} = W + \Pi(4\phi\sqrt{\det\mathbf{M}} - s_{lower} - \beta^2). \tag{34}$$

Here Π is the Lagrange multiplier and $\beta^2(\geq 0)$ is the slack variable to ensure the satisfaction of the inequality constraint. The values of the linker length are also limited by the constraint that the linkers must be shorter than the monomer number N of the polymers. This constraint can be used to identify the solution (sol) phase, but it is not directly implemented in the free energy.

3.5. Nominal free energy density function $\hat{W}$

The nominal free energy density function $\hat{W}$ is defined as the energy per volume in the reference state, i.e., $W_{tot} = \int_{V_o}\hat{W}dV$. The conservation of monomers requires that $\int_{V_o}\phi_o dV = \int_v \phi dv$. At the reference state (i.e., dry state), $v_m\phi_o = 1$. Therefore, the nominal free energy function $\hat{W}$ is obtained as

$$\hat{W} = \frac{\overline{W}}{v_m\phi}, \tag{35}$$

or explicitly

$$\hat{W} = \frac{3kT}{8\nu_m\phi\sqrt{\det\mathbf{M}}}\left[\ln\left(\frac{8\pi\phi\sqrt{\det\mathbf{M}}}{3}\right)+\frac{M_{kk}}{4\phi\sqrt{\det\mathbf{M}}}b^2\right] + \frac{kT}{\nu_s}\left[\left(\frac{1}{\nu_m\phi}-1\right)\ln(1-\nu_m\phi)+\chi(1-\nu_m\phi)\right]-\frac{E_a}{8\nu_m\phi\sqrt{\det\mathbf{M}}} + \Pi(4\phi\sqrt{\det\mathbf{M}}-s_{lower}-\beta^2) \tag{36}$$

4. Conservation of linear momentum

We denote the stress of the gel by σ_{ij}. The conservation of linear momentum in continuum mechanics can be written as the pair of conditions

$$\sigma_{ij,j} = b_i \tag{37}$$

in the volume of the system, and

$$\sigma_{ij}n_j = t_i \tag{38}$$

on its surface. Here b_i is the body force, t_i the surface traction defined in the current state and n_i the outward normal direction of a surface in the current state. The above equilibrium equation in the volume Eq. (37) neglects the inertial term by assuming that the gel is in a quasi-static state.

A simple constitutive model for the determination of the body force in the gel is to assume that it originates only from viscous drag against the background fluid, i.e., $b_i = F_i\phi$. Here F_i is the drag force applied on one monomer particle by fluid environment due to the viscosity of the solvent and given by Stokes's law $F_i = 6\pi\eta a v_i$ (Jones, 2002), where η is the viscosity of the solvent; $a = \nu_m^{1/3}$ is the radius of one monomer particle; and v_i is the velocity of the polymer network with respect to the solvents. Therefore, the conservation of linear momentum in volume Eq. (37) assumes that the net force from the divergence of stress is proportional to the relative velocity between the gel and solvents

$$\sigma_{ij,j} = 6\pi\eta\nu_m^{1/3}\phi v_i. \tag{39}$$

It can be observed that the velocity v_i links the volume fraction of monomers ϕ, connectivity tensor $\mathbf{M}$, and stress of gel σ_{ij}; and thus a completed scheme is established. Similar equilibrium equations have been used in the THB model (Tanaka et al., 1973) and can also be understood to arise from microscopic Rouse-type dynamics (Doi and Edwards, 1986). The Stokes–Einstein formula can be used to relate the factor of proportionality between stress and relative velocity v_i to the diffusion constant D of the monomers in solution via $D = kT/(6\pi\eta\nu_m^{1/3})$.

5. Stress in physical gels

We select a material particle that occupies spatial position $\mathbf{x}$ at time t and consider a field of virtual displacements $\delta\mathbf{x}$ under which there is no cross-links reformation. Based on Eqs. (17) and (19), the virtual mapping function is given by

$$\delta f_{ij} = \delta_{ij} + \frac{\partial\delta x_i}{\partial x_j}. \tag{40}$$

The connectivity tensor $\mathbf{M}$ and the number density of monomers ϕ at the virtual state $\mathbf{x}+\delta\mathbf{x}$ are given by

$$\mathbf{M}(\mathbf{x}+\delta\mathbf{x},t) = \delta\mathbf{f}\cdot\mathbf{M}(\mathbf{x},t)\cdot\delta\mathbf{f}^T \tag{41}$$

and

$$\phi(\mathbf{x}+\delta\mathbf{x},t) = \frac{\phi(\mathbf{x},t)}{\det(\delta\mathbf{f})}. \tag{42}$$

Thus free energy density W at state $\mathbf{x}+\delta\mathbf{x}$ can be obtained by plugging Eqs. (41) and (42) into Eq. (24), i.e., $W = W(\mathbf{x}+\delta\mathbf{x},t)$.

Associated with this virtual displacement field, the body force and the surface traction do work and cause the change of the free energy density via

$$\delta U = \int_v b_i\delta x_i dv + \int_a t_i\delta x_i da = \int_v \overline{W}(\mathbf{x}+\delta\mathbf{x},t)dv, \tag{43}$$

where dv is the element volume and da is the element area, in the current state; and the modified free energy density $\overline{W}$ is given by Eq. (34). Insert the conservation of linear momentum Eqs. (37) and (38) into Eq. (43) and applying the Gaussian divergence theorem, the work δU can be expressed as

$$\delta U = \int_v \sigma_{ij}\delta\varepsilon_{ij}dv. \tag{44}$$

Consequently, the stress σ_{ij} is the thermodynamic variable conjugate to the strain ε_{ij}. Let the virtual displacement to be infinitesimal, i.e., $\delta\mathbf{x}=0$. The stress is expressed as

$$\sigma_{ij}=\left.\frac{\partial\overline{W}(\mathbf{x}+\delta\mathbf{x},t)}{\partial\varepsilon_{ij}}\right|_{\delta\mathbf{x}=0}. \tag{45}$$

Explicitly, we obtain

$$\sigma_{ij}=\frac{3\phi kT}{s^2b^2}M_{ij}+\frac{kT}{\nu_s}\left[\ln(1-\nu_m\phi)+\nu_m\phi+\chi\phi^2\nu_m^2\right]\delta_{ij}. \tag{46}$$

The first term in Eq. (46) is the contribution from the deformation of the network, while the second term is the typical contribution from the regular solution model. It should be pointed out here that since the number of cross-links remains constant under the virtual displacement field $\delta\mathbf{x}$, the activation energy E_a does not explicitly appear in this expression for the stress $\boldsymbol{\sigma}$, but implicitly affects stress through $\mathbf{M}$ and ϕ.

When the number of monomers s per cross-link or number of cross-links q is fixed, the physical gels degenerate to chemical gels. Appendix B shows that the stress evaluated in Eq. (46) gives the correct limit for chemical gels when the bonds are fixed (e.g., Rubinstein and Colby, 2003; Hong et al., 2008).

6. Dimensional analysis

It is useful to reduce the number of parameters of the model by assuming that the characteristic size of all components of the model, monomers and solvent molecules is the same, i.e., $\upsilon_m=\upsilon_s=\upsilon$. This approximation entails only small corrections to the free energy density and is commonly used (e.g., Hong et al., 2008). We retain some of the molecular details of the system by using the aspect-ratio parameter $\alpha=\upsilon/b^3$. This parameter compares the volume occupied by a monomer and the volume of a cube with sizes equal to the Khun length. The aspect ratio is largest for polymers that have large side structures. In this paper we use a value for this aspect ratio of $\alpha=30$. The energy (e.g., E_a) is normalized by kT and the energy density (or stress) is normalized by kT/ν. At room temperature, $kT=4\times10^{-21}$ J and a representative value of ν is the volume of a water molecule, approximately 10^{-28} m^3. The activation energy E_a/kT varies from 2.5 (Jones, 2002) to 250 (Emsley, 1980) depending on the type of physical bonding, i.e., hydrogen bonds versus van der Waals bonding. In the paper we consider only values of the bond energy with $E_a/kT>10$. The number of monomers per chain varies in a very wide range, from 10^1 to 10^8. In the following calculation, we use a minimum link length of $s_{lower}=100$. These parameters used have been chosen to best exhibit interesting features of the model, such as the clear transition between sol and gel states. We note that the value of the aspect ratio α is relatively large and that the bonding energies consider here are strong. When a more complete choice of parameters and further model details are included, these quantities can be chosen closer to experimentally relevant values. More detailed versions of the model would consider, for example, different connectivity structures, more complex elastic models for the polymer cross-linkers.

This model has an intrinsic time scale τ_{re}. When the system considered has finite volume, the length dimension or the characteristic size of the problem, L, enters the picture and introduces another time scale $\tau_{diff}=L^2/\mathrm{D}$, which can be used to normalize time. Thus the length dimension and velocity will be normalized by L and L/τ_{diff}, respectively. The interplay between the intrinsic time scale τ_{re} and the diffusion-induced time scale τ_{diff} can be understood by normalizing the evolution law of the connectivity tensor $\mathbf{M}$ (Eq. 23) as

$$\frac{\partial\mathbf{M}}{\partial\bar{t}}=2\frac{\partial\boldsymbol{\varepsilon}}{\partial\bar{t}}\cdot\mathbf{M}+\frac{\tau_{diff}}{\tau_{re}}(\mathbf{M}-m_\phi 1), \tag{47}$$

where $\bar{t}=t/\tau_{diff}$ is the normalized time. When τ_{re} is comparable to τ_{diff}, both the contributions from the deformation and the reconstructions are important; when τ_{re} is much greater than τ_{diff}, in other words, the reconstruction occurs in much a slower rate than diffusion, $\mathbf{M}$ solely depends on the deformation. The latter degenerates to the case of chemical gel, in which the reconstruction is suppressed.

7. Free swelling of physical gels

We now apply our formalism to the problem of the swelling of a gel without constraints in a solvent. When the physical gels swell without constraints, the final equilibrium state is isotropic described by a homogeneous isotropic connectivity tensor $\mathbf{M}=m_{eq}1$ and constant ϕ. Their values are determined by

$$\begin{aligned}&\frac{\partial\hat{W}}{\partial\phi}=0\\&\frac{\partial\hat{W}}{\partial m}=0,\end{aligned} \tag{48}$$

and the inequality constraint is ensured by $\partial\hat{W}/\partial\Pi=0$. Therefore, the state of free swelling gel can be determined by solving these three nonlinear equations. Eliminating E_a from Eq. (48), one can arrive at this equation

$$\frac{3\nu}{16\phi m^2b^2}+\left[\ln(1-\nu\phi)+\nu\phi+\chi\nu^2\phi^2\right]=0. \tag{49}$$

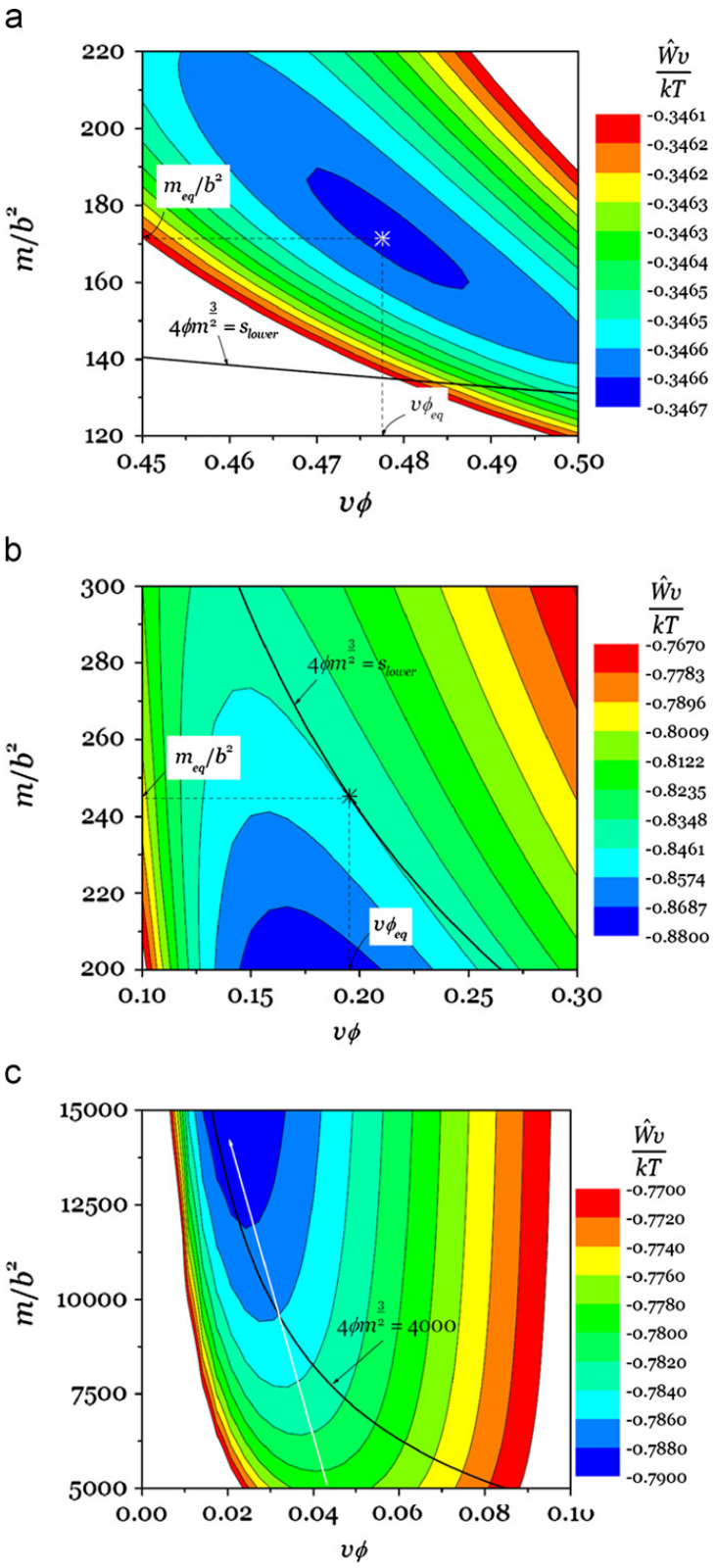

Fig. 4. Contour plots of the strain energy density function $\hat{W}/kT$ with respect to $\upsilon\phi$ and m/b^2 in un-constrained swelling. (a) The minimal energy (marked as $*$) occurs in an area satisfying the inequality constrain $4\phi m^{3/2} < s_{lower}$ for E_a/kT=28.5 and χ=0.7; (b) the minimal energy occurs at the equality constraint $4\phi m^{3/2} < s_{lower}$ for relatively strong bond energy E_a/kT=60 and χ=0.7; (c) the minimal energy is reached for vanishing $\upsilon\phi$ and infinite m/b^2 when the bond energy is relatively weak (E_a/kT=15).

This is the stress (Eq. 46) in the isotropic state; so that the free swelling means a stress-free swelling state. Instead of solving these nonlinear equations, the free swelling can be determined by minimizing the free energy density $\hat{W}(m,\phi)$ with the inequality constraint $4\phi m^{3/2} \geq s_{lower}$.

Pictorial interpretation of this constrained minimization can be shown in the contour plots of $\hat{W}(m,\phi)$ and $4\phi m^{3/2}$. Fig. 4a shows the energy contour for E_a/kT=28.5 and χ=0.7. The energy contours are closed curves and the minimal energy is found at $\upsilon\phi_{eq}$=0.478 and m_{eq}/b^2=171.4. For relatively strong bond energy, E_a/kT=60 and χ=0.7, the contours are plotted in Fig. 4b. Different from the energy contour shown in Fig. 4a, which are closed curves, the contour plots are open curves and concave downwards. The tangential point of the $\hat{W}(m,\phi)$ contour and the $4\phi m^{3/2} \geq s_{lower}$ curve is marked by an asterisk with $\upsilon\phi_{eq}$=0.51 and m_{eq}/b^2=130.1. This is the critical point with the minimal energy under the inequality constraint. This result indicate that for the current set of parameters with relative strong bond energy E_a, polymer chains tend to form the maximum allowable bonds to efficiently reduce the energy so that the minimal energy occurs at the equality constraint. Fig. 4c shows the contour plots of $\hat{W}/kT$ with relative weak bond energy E_a/kT=15 and χ=0.2, as well as $4\phi m^{3/2} = 4000$. The contour plot of $\hat{W}/kT$ does not contain a minimum value. The white line indicates a trend: as the energy $\hat{W}/kT$ further decreases, the equilibrium values of $\upsilon\phi_{eq}$ and m/b^2 approach 0 and infinity, respectively. More explicitly, the equilibrium value of s, the number of monomers between two cross-links, is infinity and the equilibrium state is a polymer solution. Based on Eq. (39), large m/b^2 makes elastic and bond energies vanishing so that the current model recovers to the solution theory, i.e., the equilibrium polymer concentration $\upsilon\phi_{eq}$ is solely determined by the mixing energy. It should be pointed out that to rigorously degenerate to the solution theory, the mixing energy (Eq. (31)) should also incorporate this term, $(kT/v_s)(v_m\phi/N)\ln(v_m\phi/N)$ to include the entropy from unconfined polymer chains, where N is the number of monomers per polymer chain. In this case, the bond activation energy or bond energy is too weak to hold the polymer chains together so that all cross-links are broken and the vectors defining the connectivity tensor do not exist. In other words, the gel dissolves into a polymer solution.

Fig. 5 shows the effect of the activation energy on the equilibrium polymer concentration. A phase transition is observed, at which the equilibrium polymer concentration has a sharp change. There always exists a critical activation energy at which the phase transition from solution to gel occurs. For relatively hydrophobic polymers (e.g., χ=0.7), the phase transition occurs at a relatively weak activation energy. For relatively hydrophilic polymers (χ=0.5, 0.2), the mixing energy prefers to dissolve the polymer, but this effect is balanced with a relative strong activation energy. One can also observe a phase transitions when the interaction parameter χ has a sudden change. The phase transition can be classified to sol–gel transition and gel–gel transition. The occurrence of different type of phase transition strongly depends on the activation energy. These phase transitions, sol–gel transition (Tempel et al., 1996; Jeong et al., 1999, 2002) and gel–gel transition (Hirokawa and Tanaka, 1984; Bae et al., 1991) have been extensively observed in experiments. The change of E_a/kT and χ can be realized by variations of the temperature. In other words, there exists a critical temperature at which the phase transition occurs in the macroscopic state. This behavior has been extensively observed in thermoreversible gels (such as PNIPAAm gel) (Ono et al., 2007).

The phase behavior is also illustrated for fixed activation energy and various χ as shown in Fig. 6. For a weak activation energy (e.g., E_a/kT=15), only the sol state is present. The gel state is present when the activation energy is relatively strong (e.g., E_a/kT=60). The sol–gel transition occurs at the moderate activation energy (e.g., E_a/kT=30, 40, and 50).

The previous results assume that the polymer is trapped in a region from which solvent can enter or exit without energetic penalty. These fluxes change the area of the interface between the gel and the pure solvent region and it is

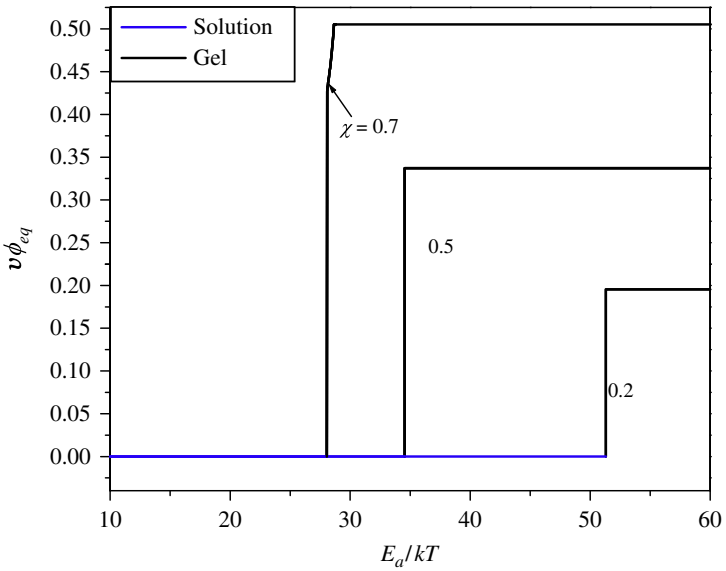

Fig. 5. The final equilibrium state of the free-swelling gel can be a sol or gel state. The gel state has a specific density value while the monomer density of the sol state can be considered to have zero monomer density. The graph shows the equilibrium state of the system. When the equilibrium state is a gel, the monomer density is shown. The equilibrium state is shown as a function of the activation energy E_a/kT for various values of the χ parameter.

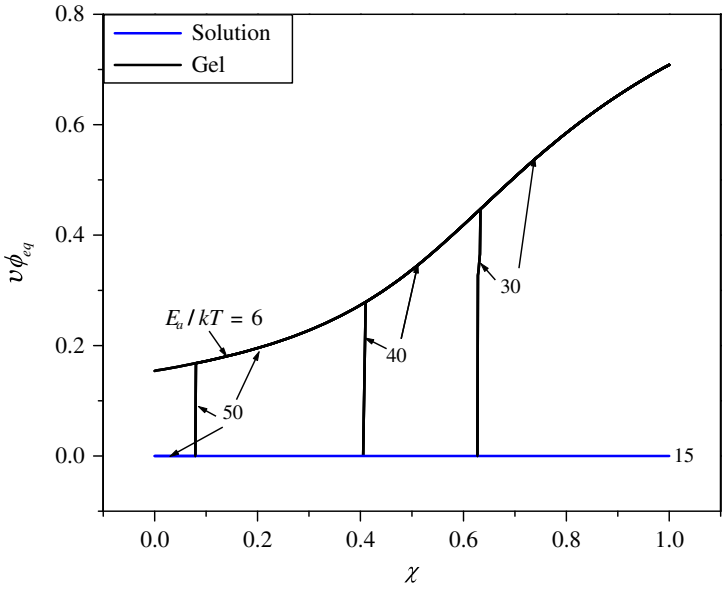

Fig. 6. As in Fig. 5, the graph shows the equilibrium state of a free swelling gel, as a function of the χ parameter for various values of the activation energy E_a/kT.

assumed that there is no cost to this area change. In this scenario the condition for equilibrium is the balance of osmotic pressure in the gel and the outside environment (Eq. $(48)_1$) but not the balance of the chemical potential of monomers. This scenario is approximately realizable with a proper selection of boundary material, such as an extremely flexible, solvent-permeable but monomer-impermeable balloon. However, a more interesting case in experiments is when the gel is in direct contact with the solvent and is not constrained by an interface. In this second case, the gel is in fact in equilibrium with a dilute polymer phase. The conditions for equilibrium are that both osmotic pressure and chemical potential be equal in both phases. We examine these now in more detail.

It can be shown that the osmotic pressure for a very dilute polymer solution can be approximately taken to be zero since it is, to first order, proportional to concentration of polymer. On the other hand, the osmotic pressure of the gel is proportional to $\partial\hat{W}/\partial\phi$. Thus, the equilibrium of osmotic pressures is well approximated by Eq. $(48)_1$.

Next, the chemical potential of the monomers is obtained as the derivative of the free energy density $\overline{W}$ (per current volume) with respect to the number density of monomer ϕ. In the dilute phase the chemical potential contains a term proportional to the logarithm of concentration $\ln(v_m\phi/N)$. This term is highly sensitive to concentration. When a gel is immersed in a solvent and the solvent region is not several orders of magnitude larger than the size of the gel, the chemical potential condition can be quickly satisfied. The gel can release a small fraction of its polymer chains into the surrounding solution thus changing the environment concentration and the chemical potential of the solvent phase. Eventually the chemical potential is equilibrated, at the cost of a small polymer chain number change. We conclude that the equilibrium conditions for free swelling and coexistence with a dilute solvent lead to essentially identical solutions.

The only caveat to this broad rule is that when the minimum of the constrained problem for free swelling is found to correspond to a solvent phase ($s > N$). In such case, the true equilibrium state of the system is a single homogenous dilute phase instead of coexistence of two separate phases.

With the identification outlined above, we can now qualitatively compare our results for the free swelling problem with experimental determinations of the coexistence region of the phase diagram of specific physical gels. We consider, in particular, the case of copolymers with a majority of NIPAAm monomers (Leon et al., 2009) that have been extensively used in drug delivery. For these materials, several prominent features appear in their phase diagrams. In the temperature-volume fraction phase diagram (Fig. 4 in Leon et al., 2009), there exists a critical temperature (i.e., LCST) at which the phase separation of sol and gel is presented. Above the LCST a system decomposes into a mixture of sol and gel states, i.e., coexistence states. In polymeric systems the key effect of temperature change is the modification of the χ parameter. For LCST type systems a larger temperature corresponds to a greater magnitude of the interaction parameter χ. By the connection made above between the free swelling problem and coexistence, we see that the features of the phase diagram closely correspond to those of our results (Fig. 6). We have a sharp onset of swelling that corresponds to the presence of the LCST and a gel/sol coexistence state above the sharp onset. This feature qualitatively agrees with the experiment of a NIPAAm based physical gel.

8. Stress driven phase transition

Many experiments have shown the so-called yielding behavior of physical gels, in which a gel changes to solution upon application of an external stress, such as the shear stress by rheometer (e.g., Kim et al., 2003; Rogovina et al., 2008;

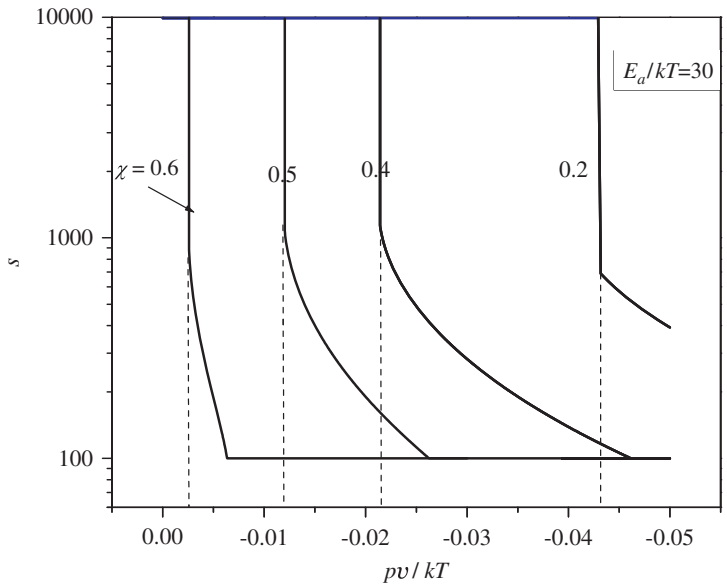

Fig. 7. Phase transition by compression. The graph shows the number of monomers between two cross linkers, s, versus the hydrostatic pressure $p\upsilon/kT$ for E_a/kT=30 and various values of the χ parameter. It is observed that a sol–gel transition occur at a critical pressure value.

Putz and Burghelea, 2009). We now study the stress driven phase transition in physical gels. A hydrostatic stress p ($p<0$ for compression and $p>0$ for tension) is applied so that the stress satisfies the following equation:

$$\frac{3\nu}{16\phi m^2 b^2}+\left[\ln(1-\nu\phi)+\nu\phi+\chi\nu^2\phi^2\right]=\frac{p\nu}{kT}. \tag{50}$$

The minimization of the free energy density with respect to the internal variable m, i.e., $\partial\hat{W}/\partial m=0$ is also required, along with the inequality constraint enforced by $\partial\hat{W}/\partial\Pi=0$, which form three nonlinear equations to determine the swelling of a physical gel under hydrostatic stress. Similar to the free swelling case, this problem can also be solved by minimizing the modified free energy density function $L=\hat{W}(m,\phi)-p/(\nu\phi)$ with the inequality constraint $4\phi m^{3/2}\geq s_{lower}$. Here the term $p/(\upsilon\phi)$ is the work done by the hydrostatic stress.

First, we study the compression induced phase transition. The number of monomers between two cross-links, s, can clearly indicate the solution or gel state. Large or infinite s denotes solution state and finite s is for gel state. Fig. 7 shows the relation between s and pressure $p\upsilon/kT$, for a given activation energy E_a/kT=30 and various χ. Critical hydrostatic pressure for the sol–gel transition depends on the hydrophilicity of the polymer. The critical pressure for gels with relative large χ is less than that with relative small χ. The mechanism for the sol–gel transition can be understood as the following. Upon compression, the monomers that are initially at the solution state are brought together. Once the monomer concentration reaches a critical value, cross-links start to form so that the phase transition occurs. The critical compressive stress for hydrophilic polymers (small χ) is greater than that for the hydrophobic ones (large χ) because the former tends to dissolve in solvent.

Next, we study the tension case. In tension, Eq. (50) can only be satisfied if the polymer is actually forming a gel. Therefore, the location of the gel–sol transition is determined by the critical point at which solutions of Eq. (50) do not exist. Fig. 8a shows the relation between s and tensile stress $p\upsilon/kT$, for an activation energy E_a/kT=60 and various χ. The transition predicted is sharp. Before the tensile stress reaches the critical point, the volume fraction of monomers $\upsilon\phi_{eq}$ decreases or equivalently the volume of the gel increases to accommodate the tensile stress $p\upsilon/kT$ without the dissociation of cross-links (Fig. 8b). Once the critical stress is reached, gel-sol phase transition is trigged and all cross-links are broken. The gel–sol transition occurs when the increase of gel volume alone cannot accommodate the deformation.

9. Concluding remarks

We have developed a phenomenological model for physical gels. A mean-field framework is used to capture the details at the microscopic level, e.g., cross-links' reformation, through a connectivity tensor **M**, and to define the measurable quantities at the macroscopic level by statistic averaging, such as the volume fraction of the monomer ϕ, number of monomers per cross-link s, and the number of cross-links per volume q. An evolution rule for the connectivity tensor **M** has been proposed that includes the effect of cross-link reformation. We have proposed a free energy density function for physical gels, which consists of three components, namely elastic energy, mixing energy, and bond energy. The free energy density function depends on two independent variables, **M** and ϕ. The equilibrium equations and the stress are derived

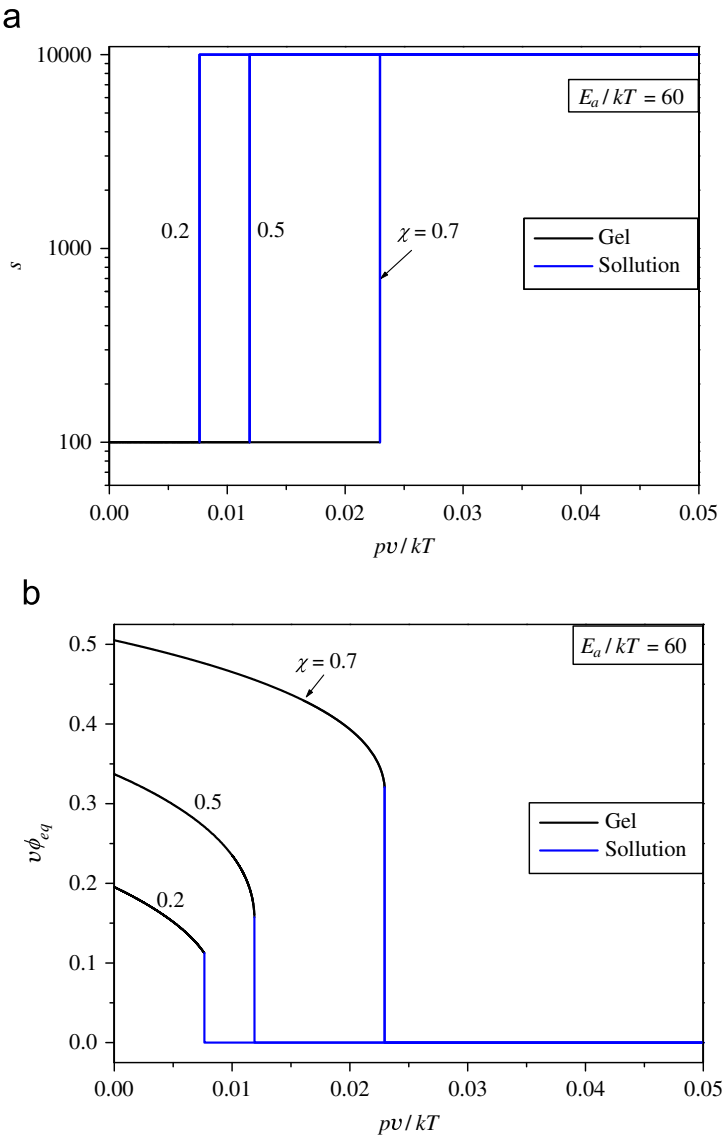

Fig. 8. Phase transition by tension. The graph shows the number of monomers between two cross linkers, s, versus the hydrostatic pressure $p\upsilon/kT$ for E_a/kT=60 and various values of the χ parameter. It is observed that a sol-gel transition occur at a critical stress value.

from the work conjugate relation at the current state. The presented framework is able to recover the case of chemical gels when the number of monomers per cross-link s is fixed.

We have examined the thermodynamic properties of this model and considered two specific conditions: the un-constrained swelling of a physical gels and its counterpart under imposed stress conditions. We have used the model to study the properties of the sol–gel transitions as a function of the bond activation energy E_a and the polymer/solvent interaction parameter χ. Our study of stress-driven behavior clearly shows the expected reformation of bonds under such conditions.

We intend to further explore other properties of physical gels that can be addressed by means of this model and its extensions. In particular, the model we have presented provides a framework for the exploration not only of the static properties of physical gels, but is constructed so as to address its dynamic properties. We have proposed a model for the evolution of the key variable of our approach, the connectivity tensor **M**. A full dynamic model will be developed in a separate publication.

Acknowledgements

YA acknowledges the financial support from the China Scholarship Council. FJS acknowledges the support from NSF DMR-0805330. HJ is grateful for financial support from NSF CMMI-0844737.

Appendix A

For chemical gels, all accessible states can be obtained by means of a map from an isotropic state. The connectivity tensor $\mathbf{M}$ at the arbitrary states is related to its counterpart $\mathbf{M}_0$ at the isotropic state via

$$\mathbf{M} = \mathbf{F}\cdot\mathbf{M}_o\cdot\mathbf{F}^T \tag{A.1}$$

where $\mathbf{F}$ is the deformation gradient, $\mathbf{F}^T$ the transpose of deformation gradient, and $\mathbf{M}_o$ is given by (similar to Eq. (6))

$$\mathbf{M}_o = \frac{1}{3}R_o^2\mathbf{I}, \tag{A.2}$$

where $\mathbf{I}$ is the second-order identity tensor. The mean-square displacement of a random walk, from one cross-link to a neighbor cross-link along a segment of a polymer chain with s monomers, is given by (Rubinstein and Colby, 2003)

$$R_o^2 = sb^2. \tag{A.3}$$

Eqs. (A.2) and (A.3) show that for chemical gel in which the number of monomers s between two cross-links is fixed, Kuhn constant b has a simple relation with the isotropic connectivity tensor $\mathbf{M}_o$. The trace of $\mathbf{M}$ is thus

$$M_{kk} = \frac{1}{3}sb^2(\lambda_1^2+\lambda_2^2+\lambda_3^2), \tag{A.4}$$

where $\lambda_i(i=1,2,3)$ are the principle stretches or the eigenvalues of the deformation gradient $\mathbf{F}$. The number of cross-link segments per volume is given by

$$n = \frac{\phi}{s}. \tag{A.5}$$

The elastic energy density for chemical gels can be obtained by substituting Eqs. (A.4) and (A.5) into the elastic energy density given by Eq. (29)

$$W_{elastic}^{\text{chemical gel}} = \frac{nkT}{2}\left[\lambda_1^2+\lambda_2^2+\lambda_3^2+3\ln\left(\frac{2\pi s}{3}\right)\right]. \tag{A.6}$$

We note that the constant term $(3nkT/2)\ln(2\pi s/3)$ is different from the one that appears in the literature (e.g., Rubinstein and Colby, 2003) since the reference states are different. We also point out that this elastic energy does not have the logarithmic term $\ln(\lambda_1\lambda_2\lambda_3)$ which was originally included in Flory's model (Flory, 1953) and recently modified by Hong et al. (2008). Deam and Edwards (1976) have discussed the reasons for the difference in these expressions. Some current theoretical literature, supported by experimental results, omits logarithmic term. See for example, Rubinstein and Colby (2003) and Han et al. (1999).

Appendix B

Eqs. (A.1) and (A.2) have shown that

$$M_{ij} = \frac{1}{3}sb^2F_{iK}F_{jK}. \tag{B.1}$$

The conservation of monomers gives

$$\phi_o = \phi\det(\mathbf{F}), \tag{B.2}$$

where the number density of monomers at the reference state (i.e., dry state) is related to monomer volume via $\phi_o v_m = 1$. Then the number of cross-link segments per volume at the reference state is given by

$$\mathcal{N} = \frac{\phi_o}{s} \tag{B.3}$$

which is used in a recent paper (Hong et al., 2008). Combining Eqs. (B.1) and (B.3) with the expression for stress, Eq. (46), we obtain the stress for chemical gels as

$$\sigma_{ij} = \frac{\mathcal{N}kT}{\det(\mathbf{F})}F_{iK}F_{jK} + \frac{kT}{v_s}\left\{\ln\left[1-\frac{1}{\det(\mathbf{F})}\right]+\frac{1}{\det(\mathbf{F})}+\frac{\chi}{\det(\mathbf{F})^2}\right\}\delta_{ij} \tag{B.4}$$

We note that the stress does not contain a term of the form $-(\mathcal{N}kT/\det(\mathbf{F}))\delta_{ij}$, which was included in Hong et al. (2008). This term is derived from the logarithmic term in the elastic energy. Appendix A discusses the omission of this term in our model.

References

Bae, Y.H., Okano, T., Kim, S.W., 1991. On off thermocontrol of solute transport 1. Temperature-dependence of swelling of *N*-isopropylacrylamide networks modified with hydrophobic components in water. Pharmaceutical Research 8 (4), 531–537.

Beck, J., Angus, R., Madsen, B., Britt, D., Vernon, B., Nguyen, K.T., 2007. Islet encapsulation: strategies to enhance islet cell functions. Tissue Engineering 13 (3), 589–599.
Beebe, D.J., Moore, J.S., Bauer, J.M., Yu, Q., Liu, R.H., Devadoss, C., Jo, B.H., 2000. Functional hydrogel structures for autonomous flow control inside microfluidic channels. Nature 404 (6778) 588-+.
Deam, R.T., Edwards, S.F., 1976. Theory of rubber elasticity. Philosophical Transactions of the Royal Society of London Series a—Mathematical Physical and Engineering Sciences 280 (1296), 317–353.
Doi, M., Edwards, S.F., 1986. The Theory of Polymer Dynamics. Oxford University Press, New York.
Emsley, J., 1980. Very strong hydrogen bonds. Chemical Society Reviews 9, 91–124.
Flory, P.I., 1942. Thermodynamics of high polymer solutions. Journal of Chemical Physics 10 (1), 51–61.
Flory, P.J., 1941. Thermodynamics of high polymer solutions. Journal of Chemical Physics 9 (8), 660–661.
Flory, P.J., 1953. Principles of polymer chemistry. Cornell University Press, Ithaca.
Han, W.H., Horkay, F., McKenna, G.B., 1999. Mechanical and swelling behaviors of rubber: a comparison of some molecular models with experiment. Mathematics and Mechanics of Solids 4 (2), 139–167.
Hirokawa, Y., Tanaka, T., 1984. Volume phase-transition in a nonionic gel. Journal of Chemical Physics 81 (12), 6379–6380.
Hong, W., Zhao, X.H., Zhou, J.X., Suo, Z.G., 2008. A theory of coupled diffusion and large deformation in polymeric gels. Journal of the Mechanics and Physics of Solids 56 (5), 1779–1793.
Huggins, M.L., 1941. Solutions of long chain compounds. Journal of Chemical Physics 9 (5), 440.
Jeong, B., Bae, Y.H., Kim, S.W., 1999. Thermoreversible gelation of PEG-PLGA-PEG triblock copolymer aqueous solutions. Macromolecules 32 (21), 7064–7069.
Jeong, B., Bae, Y.H., Lee, D.S., Kim, S.W., 1997. Biodegradable block copolymers as injectable drug-delivery systems. Nature 388 (6645), 860–862.
Jeong, B., Kim, S.W., Bae, Y.H., 2002. Thermosensitive sol–gel reversible hydrogels. Advanced Drug Delivery Reviews 54 (1), 37–51.
Jones, R.A.L., 2002. Soft Condensed Matter. Oxford University Press, New York.
Kim, J.Y., Song, J.Y., Lee, E.J., Park, S.K., 2003. Rheological properties and microstructures of Carbopol gel network system. Colloid and Polymer Science 281 (7), 614–623.
Lee, B.H., West, B., McLemore, R., Pauken, C., Vernon, B.L., 2006. In-situ injectable physically and chemically gelling NIPAAm-based copolymer system for embolization. Biomacromolecules 7 (6), 2059–2064.
Lee, K.Y., Mooney, D.J., 2001. Hydrogels for tissue engineering. Chemical Reviews 101 (7), 1869–1879.
Leon, C., Solis, F.J., Vernon, B., 2009. Phase behavior and shrinking kinetics of thermo-reversible poly(*N*-isopropylacrylamide-2-hydroxyethyl methacrylate). Materials Research Society Symposia Proceedings, 1190.
Ono, T., Sugimoto, T., Shinkai, S., Sada, K., 2007. Lipophilic polyelectrolyte gels as super-absorbent polymers for nonpolar organic solvents. Nature Materials 6 (6), 429–433.
Prigogine, I., 1967. Introduction to Thermodynamics of Irreversible Processes. Wiley, New York.
Putz, A.M.V., Burghelea, T.I., 2009. The solid-fluid transition in a yield stress shear thinning physical gel. Rheologica Acta 48 (6), 673–689.
Qiu, Y., Park, K., 2001. Environment-sensitive hydrogels for drug delivery. Advanced Drug Delivery Reviews 53 (3), 321–339.
Rogovina, L.Z., Vasil'ev, V.G., Braudo, E.E., 2008. Definition of the concept of polymer gel. Polymer Science Series C 50 (1), 85–92.
Rubinstein, M., Colby, R.H., 2003. Polymer Physics. Oxford University Press.
Sidorenko, A., Krupenkin, T., Taylor, A., Fratzl, P., Aizenberg, J., 2007. Reversible switching of hydrogel-actuated nanostructures into complex micropatterns. Science 315 (5811), 487–490.
Solis, F.J., Weiss-Malik, R., Vernon, B., 2005. Local monomer activation model for phase behavior and calorimetric properties of LCST gel-forming polymers. Macromolecules 38, 4456–4464.
Suzuki, A., Yoshikawa, S., Bai, G., 1999. Shrinking pattern and phase transition velocity of poly(*N*-isopropylacrylamide) gel. Journal of Chemical Physics 111 (1), 360–367.
Tanaka, T., Hocker, L.O., Benedek, G.B., 1973. Spectrum of light scattered from a viscoelastic gel. Journal of Chemical Physics 59 (9), 5151–5159.
Tempel, M., Isenberg, G., Sackmann, E., 1996. Temperature-induced sol-gel transition and microgel formation in alpha-actinin cross-linked actin networks: a rheological study. Physical Review E 54 (2), 1802–1810.